



Missouri University of Science and Technology  
Scholars' Mine

Mechanical and Aerospace Engineering Faculty  
Research & Creative Works

Mechanical and Aerospace Engineering

01 Aug 2019

## Predictive Model for Thermal and Stress Field in Selective Laser Melting Process – Part II

Lan Li

Lei Yan

Yitao Chen

Tan Pan

*et. al.* For a complete list of authors, see [https://scholarsmine.mst.edu/mec\\_aereng\\_facwork/4478](https://scholarsmine.mst.edu/mec_aereng_facwork/4478)

Follow this and additional works at: [https://scholarsmine.mst.edu/mec\\_aereng\\_facwork](https://scholarsmine.mst.edu/mec_aereng_facwork)

 Part of the [Mechanical Engineering Commons](#)

### Recommended Citation

L. Li et al., "Predictive Model for Thermal and Stress Field in Selective Laser Melting Process – Part II," *Procedia Manufacturing*, vol. 39, pp. 547-555, Elsevier B.V., Aug 2019.

The definitive version is available at <https://doi.org/10.1016/j.promfg.2020.01.416>



This work is licensed under a [Creative Commons Attribution-Noncommercial-No Derivative Works 4.0 License](#).

This Article - Conference proceedings is brought to you for free and open access by Scholars' Mine. It has been accepted for inclusion in Mechanical and Aerospace Engineering Faculty Research & Creative Works by an authorized administrator of Scholars' Mine. This work is protected by U. S. Copyright Law. Unauthorized use including reproduction for redistribution requires the permission of the copyright holder. For more information, please contact [scholarsmine@mst.edu](mailto:scholarsmine@mst.edu).



Available online at [www.sciencedirect.com](http://www.sciencedirect.com)

**ScienceDirect**

Procedia Manufacturing 39 (2019) 547–555

**Procedia**  
MANUFACTURING

[www.elsevier.com/locate/procedia](http://www.elsevier.com/locate/procedia)

25th International Conference on Production Research Manufacturing Innovation:  
Cyber Physical Manufacturing  
August 9-14, 2019 | Chicago, Illinois (USA)

## Predictive Model for Thermal and Stress Field in Selective Laser Melting Process—Part II

Lan Li\*, Lei Yan, Yitao Chen, Tan Pan, Xinchang Zhang, Wenyuan Cui, Aaron Flood,  
Frank Liou

*Missouri University of Science and Technology, 205 W 12th St, Rolla, MO, 65401, USA*

---

### Abstract

Finite Element Analysis (FEA) is used to predict the transient thermal cycle and optimize process parameters to analyze these effects on deformation and residual stresses. However, the process of predicting the thermal history in this process with the FEA method is usually time-consuming, especially for large-scale parts. In this paper, an effective predictive model of part deformation and residual stress was developed for accurately predicting deformation and residual stresses in large-scale parts. An equivalent body heat flux proposed from the single layer laser scan model was imported as the thermal load to the layer by layer model. The hatched layer is then heated up by the equivalent body heat flux and used as a basic unit element to build up the macroscale part. The thermal history and residual stress fields of two solid parts with different support structures during the SLM process were simulated. Layer heat source method has the capability for fast temperature prediction in the SLM process, while sacrificing modeling details for the computational time-saving purpose. Thus numerical modeling in this work can be a very useful tool for the parametric study of process parameters, residual stresses and deformations.

© 2019 The Authors. Published by Elsevier Ltd.

This is an open access article under the CC BY-NC-ND license (<https://creativecommons.org/licenses/by-nc-nd/4.0/>)

Peer-review under responsibility of the scientific committee of the ICPR25 International Scientific & Advisory and Organizing committee members

*Keywords:* SLM; finite element analysis; layer heat source model; distortion; residual stress

---

\* Corresponding author. Tel.: +1-573-612-9152

E-mail address: [ll752@mst.edu](mailto:ll752@mst.edu)

2351-9789 © 2019 The Authors. Published by Elsevier Ltd.

This is an open access article under the CC BY-NC-ND license (<https://creativecommons.org/licenses/by-nc-nd/4.0/>)

Peer-review under responsibility of the scientific committee of the ICPR25 International Scientific & Advisory and Organizing committee members

10.1016/j.promfg.2020.01.416

## 1. Introduction

In the selective laser melting (SLM) process, transient temperature fields are important for microstructure evolution, residual stress and distortion analyses. Many efforts had been put on the temperature field analysis and were mainly based on the finite element analysis (FEA) method [1-4] in order to have a fundamental study of the stress mechanism at the micro part level. The traditional single track or single layer modeling of predicting the thermal history with the FEA method is usually time-consuming, especially for large-scale parts. In Part I, the prediction of thermal stress for several tracks at the microscale part using a fine mesh would take several hours to complete. Moreover, a practical part may require hundreds or thousands of layers in SLM process and dramatically increases the computational time. Therefore, it is extremely difficult to predict part distortion of a practical SLMed part if every single track or pulse is modeled even using a powerful workstation.

Herein, methods called, track-heat-source, layer-heat-source and volume-heat-source are proposed for fast prediction of transient thermal history and residual stress field in large-scale part fabrication via the SLM process. Here a representative surface heat flux or body heat flux is applied to a target surface or an entire layer for a representative time rather than simulating every single laser pulse. The simplification of a local laser heating process to a uniform distributing heat source was made. The magnitude of the heat flux and the application time depend on the machine specific process parameters, like laser power and scanning speed. This method speeded up the simulation time without compromising the accuracy of the prediction of deformation and thermal stresses in the AM process [5-7]. Li et al. [8] developed a multiscale modeling approach with layer by layer heat source to effectively predict residual stress and part distortion of a twin cantilever. The hatched layer is heated up by an equivalent body heat flux and used as a basic unit to build up the macroscale part in a layer by layer fashion. The thermal history and residual stress fields of the twin cantilever during the SLM process were analyzed. The simulated cantilever distortion agreed with the measured data with reasonable accuracy. Michael F. Zaeh and Gregor Branner [9] numerically calculated the residual stresses and deformations results for a cantilever geometry using a volume by volume heat source. The simulation was carried out with the simplification of increasing the layer thickness to 1.0 mm instead of 50  $\mu\text{m}$  within the real process in order to reduce the required simulation time.

In this paper, a novel concept of layer heat source model for SLM process with the performed material of SS304L was developed for accurately predicting thermal history, distortion and residual stress with low computational cost and acceptable accuracy. The hatched layer was heated up layer by layer using a body heat flux to build up the largescale part. The thermal load applied in this work was calculated from the microscale model in part I. The thermal history and residual stress fields of two solid parts with different support structures during the SLM process were simulated. Layer heat source method has the capability for fast temperature prediction in the SLM process, while sacrificing modeling details for the computational time-saving purpose. The numerical modeling in this work can be a very useful tool for the parametric study of process parameters, residual stresses and deformations.

## 2. Thermo-mechanical analysis of selective laser melting 304L stainless steel

The coupled thermo-mechanical multiscale method is described as follows: First, the transient thermal analysis is calculated. Then the computed temperature results are used for the mechanical calculations as the thermal load to calculate the thermal stress and deformation. The hatched layer is heated up layer by layer using a body heat flux to build up the largescale part rather than simulating every single laser pulse. The element birth and death function is used to activate or deactivate an element. At the start of the simulation, the substrate elements were all activated. The elements of the new layer were activated sequentially to simulate material addition process. The other simulation conditions, like process parameters, material properties and boundary conditions are also the same with one layer SLM simulation in Part I. The total computational time can be dramatically reduced using this approach compared with that in the conventional modeling methods.

Considering the computational time, the layer-heat-source method took about 30 minutes compared with the conventional method that took about several hours for the singer layer multi-tracks model in Part I on a computer with an Intel(R) E5-2620V2 Processor 2.1 GHz and 64.0 GB RAM hardware. The rougher the prediction model is implemented, the less computational time is needed and thus sacrificing the accuracy of the results.

## 2.1. Modeling of part dimensions and mesh

In this model, the process of building two solid cubes with different support structures was modeled. The whole configuration is just modeled in half, as the part is symmetrical. The dimensions of the cubic (half model) are 25 mm (length)  $\times$  7.5 mm (width)  $\times$  10 mm (height). The elements of the cube are hexahedral elements with 0.1 mm (length)  $\times$  0.1 mm (width)  $\times$  0.1 mm (height). Two support structures with a thickness of 3 mm and different shapes are described in Figure 1 (b) and 1 (c). Figure 1 (b) and 1 (c) show the solid layer support structure and cantilever beam support structure. These two support structures have the same mesh density with the cube. The substrate is also symmetric and large enough to eliminate the boundary effect. The initial temperatures of both the powder bed and the substrate were set to 25°C. The bottom surface of the substrate was fixed during the SLM process. Usually, all nodes at the bottom region were rigidly constrained as no deformation occurred during the SLM process. The finite element model used a fixed mesh size for all the substrates, support structures and depositions during simulation. To simulate the addition of the material layer, the element birth and death function was used to activate or deactivate an element. The element death function was used to deactivate an element by setting its stiffness to zero, while the element birth function was used to activate an element by setting the right stiffness value. At the start of the simulation, the substrate elements were all activated. However, the deposited elements were activated sequentially to simulate new layer material addition. The simulation was carried out in this work with the simplification of increasing the layer thickness to 100  $\mu\text{m}$  instead of 50  $\mu\text{m}$  within the real process in order to reduce the required simulation time.

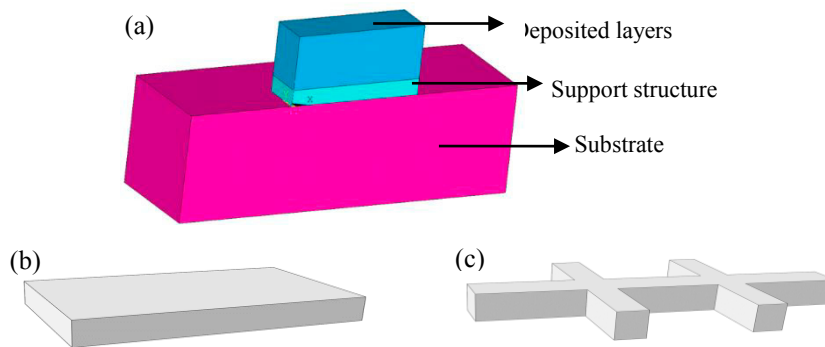


Fig. 1. (a) FEA model geometry with the simplified substrate, deposited layers and support structure; (b) solid support structure; (c) cantilever beam support structure

## 2.2. Modeling of heat flux

The hatched layer is heated up by an equivalent body heat flux and used as a basic unit to build up the part, which is described in Figure 2. The equivalent body heat flux  $q$  was developed by Li et. [8] in Equation (1). In this equation, laser power  $P$  (200W), laser absorption coefficient  $\alpha$  (0.7), laser spot diameter  $d$  (150  $\mu\text{m}$ ), melt pool depth  $t$  (100  $\mu\text{m}$ ), the melt pool depth is the distance from the bottom of the melt pool to the top surface of the layer. This value was obtained from paper [10], which was already validated by experimental study. Another term is scan hatch spacing  $Hs$  (105  $\mu\text{m}$ ). Thus the calculated  $q$ , in this case, was approximately  $11.11 \times 10^{12} \text{ W/m}^3$ . The body heat flux was applied layer by layer with the heating time of 200 microseconds. The total exposure time of the heat source in the large-scale model was obtained from converges study. The exposure time we set in the large-scale model was based on the thermal history, which can make the same maximum temperature with the maximum temperature that was calculated from the microscale laser scan model in Part I.

$$q = \frac{\alpha \cdot P}{d \cdot Hs \cdot t} \quad (1)$$

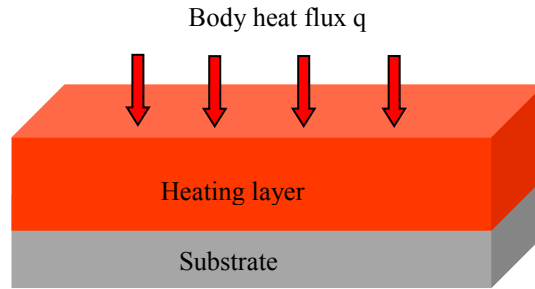


Fig. 2. Modeling of body heat flux in the layer hatched model.

### 3. Simulation Results and Discussion

Fig. 3 (a) shows the temperature history of the layer center on the top surface of different layers, 1<sup>st</sup>, 80<sup>th</sup> and the last layer. The layer experiences several cycles of heating and cooling. The first temperature peak is caused by heating up in this layer, while the second temperature peak is due to the heating process of the subsequent layer. When we zoom in one heating and cooling cycle in Figure 3 (b), we can see that the rapid heating and cooling process of one cycle happens in just 0.01 s. The temperature changing rate of rapid heating and cooling is even higher than  $10^6$  K/s. The second peak temperature is a little higher than the melting point of SS304L (1454°C), which means the solidified layer is remelted during heating of the next layer. It is found that the last layer just experienced one heating and cooling cycle. After cooling enough long time, the whole part cools down to room temperature.

In this simulation work, the heat source is applied layer by layer, but in reality, the heat source laser beam starts from one end and moves to the other end of each track. This layer by layer method leads to every location to be heated up and reaches a peak temperature simultaneously. After certain layers, the substrate is heated up and the temperature difference caused by the uniform loading methods is reduced compared with the pulse laser.

The element birth and death method application in layer heat source with a solid layer support structure are demonstrated in Figure 3 (c), (d) and (e), respectively. Fig. 3 (c) shows the temperature distribution contour with layer heat source process where the heat flux is applied to the first layer, followed by 101<sup>st</sup> and last layer in (d) and (e). After the heat source is added to the deposited layer, five seconds of cooling time is simulated and then following the same heat source application sequenced with the subsequently deposited layer. Figure 3 (f), (g) and (h) show the same layer corresponding to Figure 3 (c), (d) and (e) with cantilever beam support structure. The predicted peak temperature from each layer is about 2400 °C using the layer heat source model. The peak temperature, in fact, has the overestimation, which comes from the lack of cooling time after each track or each laser pulse in traveling laser pulse conventional model.

The displacement distributions after the 21<sup>st</sup> layer in solid part with solid layer support structure are illustrated in Figure 4 (a) ~ (d). The longitudinal displacement, transversal displacement, normal displacement and displacement sum vector are observed respectively. In Figure 4 (a) and (b), maximum displacement in x and y direction are formed at the interface region of the substrate and building part due to shape distortion with values of 29.3  $\mu\text{m}$  and 77.4  $\mu\text{m}$ , whereas the maximum displacement in z direction is formed on the top surface away from the substrate.

The stress distributions after the 21<sup>st</sup> layer in solid part with solid layer support structure are illustrated in Figure 4 (e) ~ (h). The longitudinal stress, transversal stress, normal stress and von Mises stress are observed respectively.

Among these stresses, the longitudinal stress after the deposition of the 21<sup>st</sup> layer is the largest. And the maximum longitudinal stress is acquired on the substrate at interface region with the value of -628 MPa, which is in a compressive state, whereas compressive longitudinal stresses are formed on the substrate away from the deposition layers. This layer by layer method leads to every location to be heated up simultaneously, making the stresses in three directions do not differ a lot. Maximum tensile stresses in three directions in the building part are with values of 283 MPa, 276 MPa and 308 MPa. Shear stresses are lower compared with longitudinal displacement, normal displacement and transversal displacement.

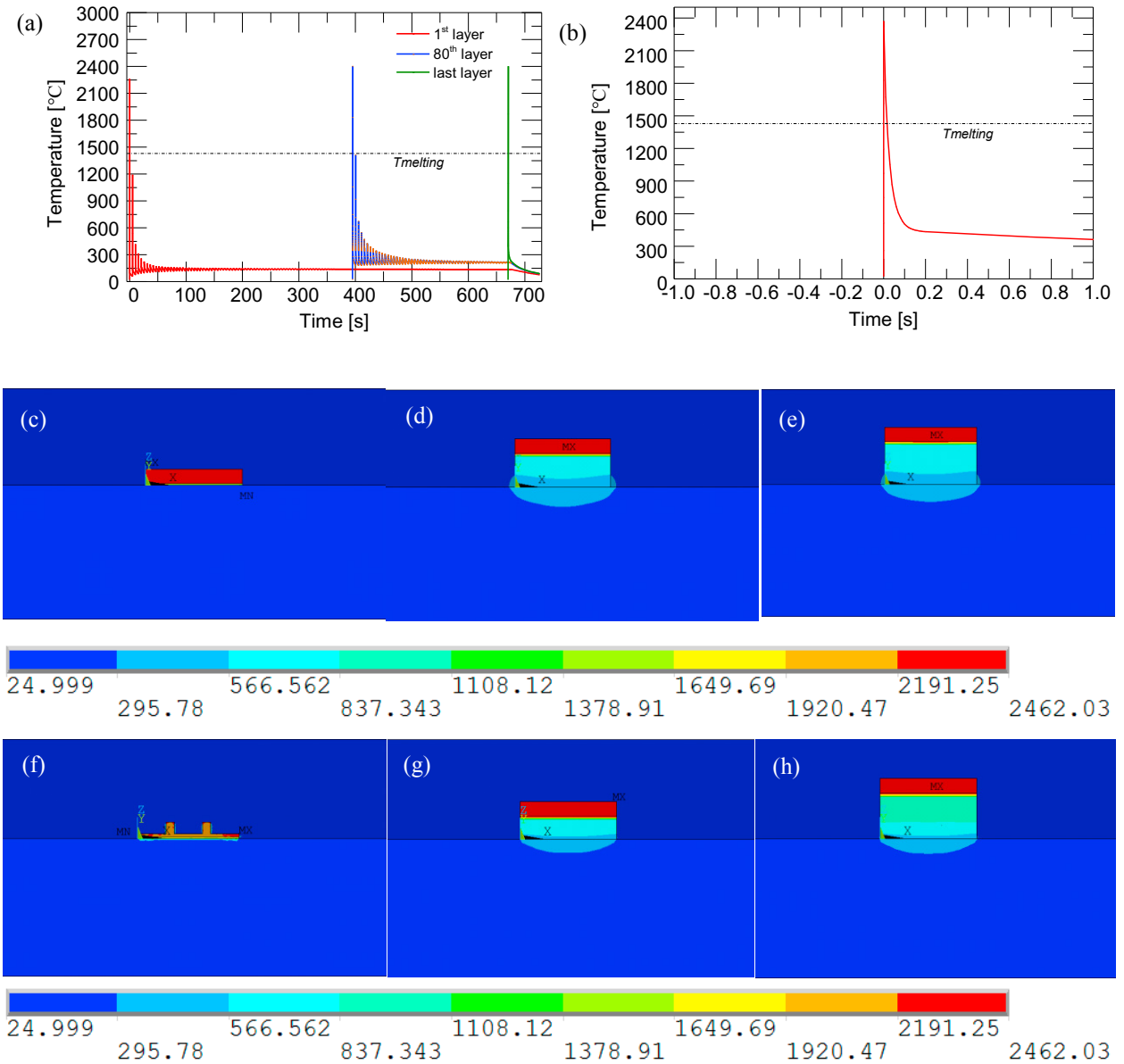


Fig. 3 (a) temperature history of the selected location on the top surface of the  $n^{\text{th}}$  layer,  $n$  is 1, 80 and last layer; (b) temperature history of the selected location in one heating and cooling cycle; temperature distribution at 1<sup>st</sup> (c), 101<sup>st</sup> (d) and last (e) layer by layer heat source with solid layer support structure; temperature distribution at 1<sup>st</sup> (f), 101<sup>st</sup> (g) and last (h) layer by layer heat source with cantilever beam support structure.

The stress distributions after the 21<sup>st</sup> layer in solid part with cantilever beam structure are illustrated in Figure 5 (a) and (b). The longitudinal stress and von Mises stress are observed respectively. The maximum compressive longitudinal stresses are formed on the substrate away from the deposition layers with the value of 156 MPa, which is much lower than that in Figure 4 (a) with the value of 628 MPa. Whereas the maximum tensile longitudinal stresses of 222 MPa is not much different with that in Figure 4 (a) with the value of 198 MPa.

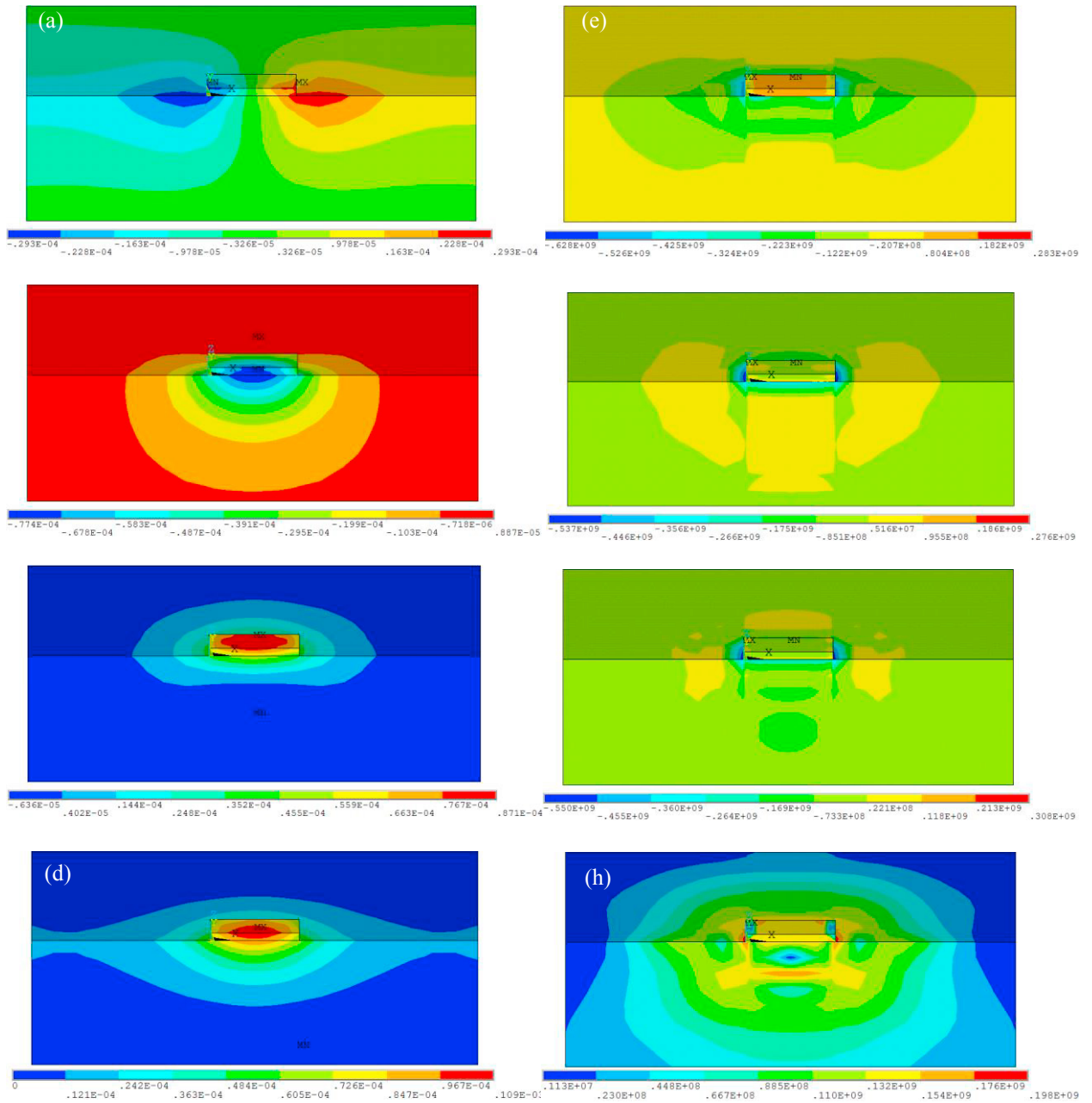


Fig. 4 (a) Longitudinal displacement,  $U_x$ , (b) transversal displacement,  $U_y$ , (c) normal displacement,  $U_z$ , (d) displacement vector sum,  $U_{sum}$ , (e) longitudinal stress,  $S_x$ , (f) transversal stress,  $S_y$ , (g) normal stress,  $S_z$ , and (h) von Mises stress,  $S_{eqv}$ , after 21st layer in solid part with solid support structure.

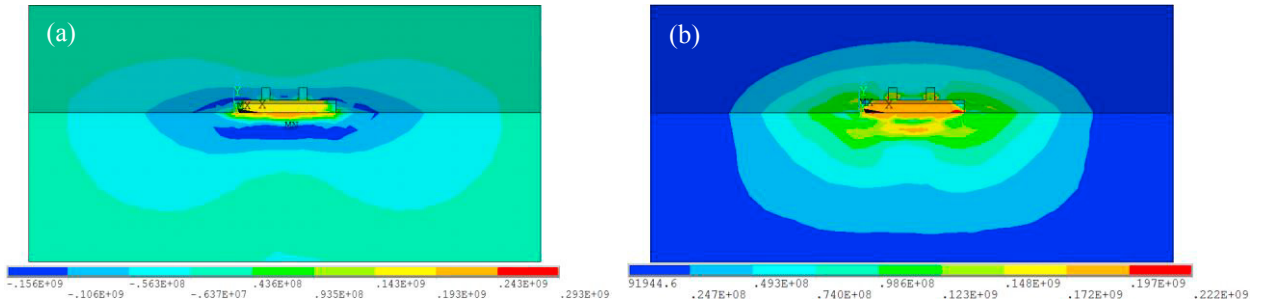


Fig. 5 (a) Longitudinal stress,  $S_x$ , (b) von Mises stress,  $Seqv$ , after the 21<sup>st</sup> layer in solid part with cantilever beam support structure.

The displacement distributions after all deposition done until cooling to room temperature in solid part with solid layer support structure are illustrated in Figure 6 (a) ~ (d). The longitudinal displacement, transversal displacement, normal displacement and displacement sum vector are observed respectively. In Figure 6 (a), maximum and minimum displacement in x direction are formed at the interface corner region of the substrate and building part, with values of  $-991 \mu\text{m}$  and  $991 \mu\text{m}$  due to shape symmetric, whereas the displacement in z direction in Figure 6 (c) is increasing from the substrate to the top surface.

Residual stress is caused due to the rapid heating and cooling during deposition in Selective Laser Melting (SLM) processes. Many researchers have studied the residual stress and revealed that two types of residual stress: compressive stress, which may cause delamination, and tensile stress, which may cause cracks. The residual stress could also introduce some deformation problems to the substrate, which is not accepted when printing a large part. The residual stress distributions after all deposition done until cooling to room temperature in solid part with solid layer support structure are illustrated in Figure 6 (e) ~ (g). The longitudinal stress, transversal stress and normal stress are observed respectively. Among these three main residual stresses, the longitudinal residual stress is the largest, with the value of  $-464\text{MPa}$ . The maximum longitudinal stress is acquired on the substrate, which is in a compressive state. Compressive longitudinal stresses are formed on the substrate near the deposition layers, making a round circle, where may cause delamination. When the residual stress is in a compressive state, it is also generally well-known that it will confer benefits for fatigue life. The presence of compressive residual stress and alternating cyclic thermal and stresses has the effect of reducing the mean stress [11]. Maximum tensile residual stresses in three directions are with values of  $339 \text{MPa}$ ,  $202 \text{MPa}$  and  $304 \text{MPa}$ .

With the numerical method for thermo-mechanical deformation and stress modeling, it is very useful for understanding the residual stress origins, thus numerical modeling in this work can be a very useful tool for the parametric study of the process parameters.

## Conclusions

The current work developed a novel concept of layer heat source model for the SLM process for accurately predicting thermal history, distortion and residual stress. The hatched layer was heated up layer by layer using a body heat flux to build up the largescale part. The thermal history and residual stress fields of two solid parts with different support structures during the SLM process were simulated. Following conclusions can be drawn from the study:

(1) Layer heat source method has the capability for fast temperature prediction in the SLM process, sacrificing modeling details for the computational time-saving purpose.

(2) Points in deposited layers undergo several thermal cycles with increasing temperature peaks because of the preheating behavior of the previous layers.

(3) The thermal deformations in different areas have apparently different characters. Maximum displacement in x direction is formed at the interface corner region of the substrate and building part, with symmetric character, whereas the displacement in z direction is increasing from the substrate to the top surface, which is much higher than the displacement in x and y direction.



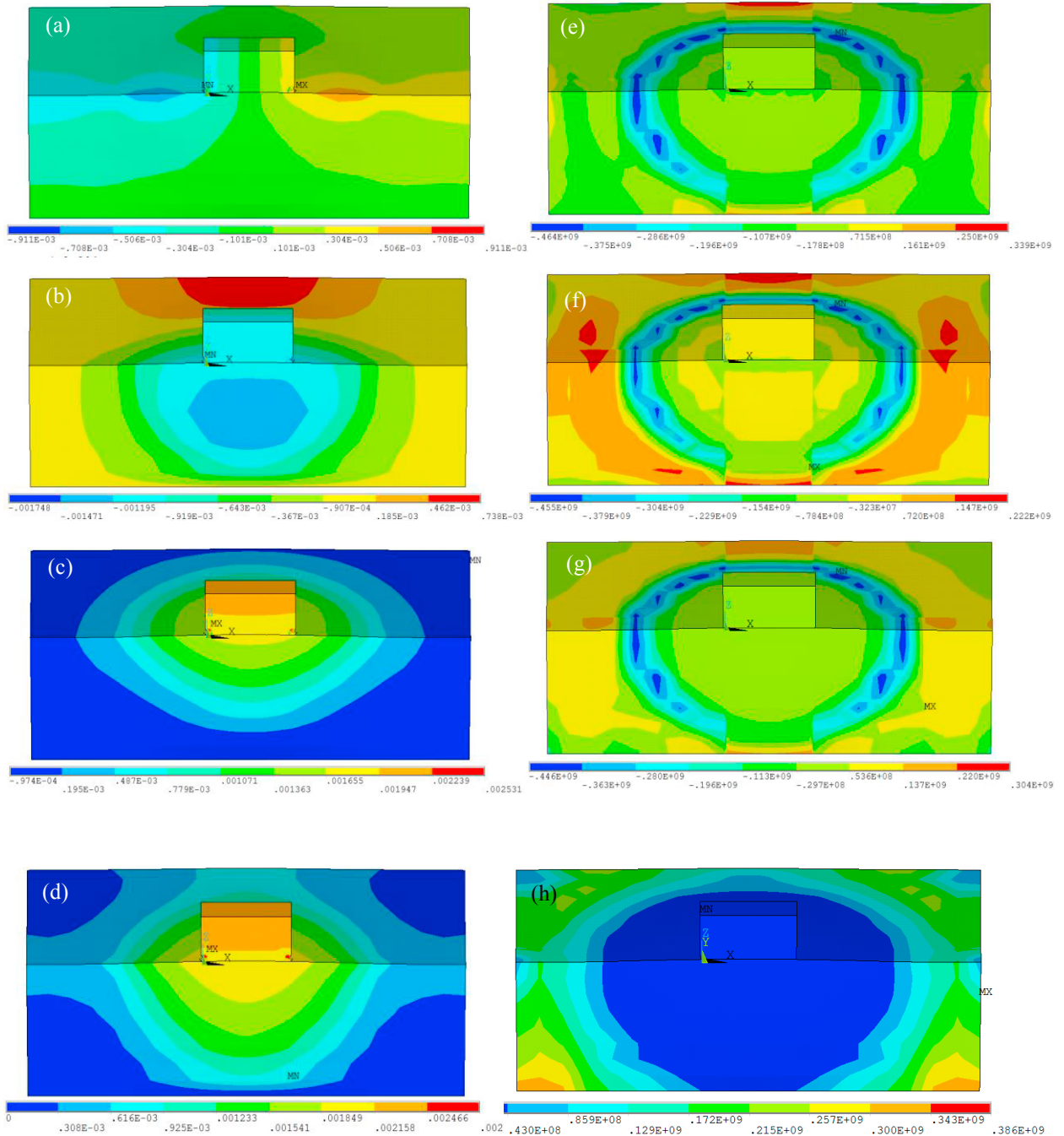


Fig. 6 (a) Longitudinal displacement,  $U_x$ , (b) transversal displacement,  $U_y$ , (c) normal displacement,  $U_z$ , (d) displacement vector sum,  $U_{sum}$ , (e) longitudinal stress,  $S_x$ , (f) transversal stress,  $S_y$ , (g) normal stress,  $S_z$ , and (h) von Mises stress,  $S_{eqv}$ , after all deposition done until cooling to room temperature in solid part with solid layer support structure.

(4) Two types of residual stress: compressive stress, which may cause delamination, and tensile stress, which may cause cracks, are caused in Selective Laser Melting (SLM) processes due to the rapid heating and cooling during deposition. The maximum longitudinal stress is acquired on the substrate, which is in a compressive state,

compressive longitudinal stresses are formed on the substrate away from the deposition layers, making a round circle. Whereas shear stresses are lower compared with longitudinal displacement, normal displacement and transversal displacement.

Layer heat source method in this work has the capability for fast temperature prediction in the SLM process. The numerical modeling in this work can be a very useful tool for the parametric study of residual stresses and deformations.

## Acknowledgements

This work was funded by Navy, proposal No.N17B-033-0066. The United States Government retains and the publisher, by accepting the article for publication, acknowledges that the United States Government retains a nonexclusive, paid up, irrevocable, worldwide license to publish or reproduce the published form of this manuscript, or allow others to do so, for the United States Government purposes. This project is led by Product Innovation and Engineering (PINE), in partnership with Missouri University of Science and Technology.

## References

- [1] P. Prabhakar, W.J. Sames, R. Dehoff, S.S. Babu, Computational modeling of residual stress formation during the electron beam melting process for Inconel 718, *Addit. Manuf.* 7 (2015) 83–91.
- [2] H.H. Zhao, G.J. Zhang, Z.Q. Yin, L. Wu, A 3D dynamical analysis of thermal behavior during single-pass multi-layer weld-based rapid prototyping, *J. Mater. Process. Technol.*, 211 (2011), pp. 488–495.
- [3] Antony, K., Arivazhagan, N., and Senthilkumaran, K., 2014, "Numerical and experimental investigations on laser melting of stainless steel 316L metal powders," *J. of Man. Proc.*, 16(3), pp. 345–355.
- [4] Y. Liu, J. Zhang, and Z. Pang, "Numerical and experimental investigation into the subsequent thermal cycling during selective laser melting of multi-layer 316L stainless steel," *Optics & Laser Technology*, vol. 98, pp. 23–32, 2018.
- [5] Keller, N., et al. "Thermo-mechanical Simulation of Additive Layer Manufacturing of Titanium Aerospace structures." *LightMAT Conference*. Vol. 3. No. 5. 2013.
- [6] Neugebauer, Fabian, et al. "Simulation of selective laser melting using process specific layer based meshing." *Proc. Fraunhofer Direct Digital Manufacturing Conf.(DDMC 2014)*, Axel Demmer, Aachen, Germany. 2014.
- [7] Lei Yan, Tan Pan, Joseph W. Newkirk, Frank Liou, Eric E. Thomas, Andrew H. Bake, James B. Castle, Fast Prediction of Thermal History in Large-Scale Parts Fabricated Via a Laser Metal Deposition Process, *Solid Freeform Fabrication 2018: Proceedings of the 29th Annual International*.
- [8] C. Li, J.F. Liu, X.Y. Fang, Y.B. Guo, Efficient predictive model of part distortion and residual stress in selective laser melting, *Additive Manufacturing*, Volume 17, October 2017, Pages 157-168.
- [9] Michael F. Zaeh, Gregor Branner, Investigations on residual stresses and deformations in selective laser melting, *Prod. Eng. Res. Devel.* (2010) 4:35–45.
- [10] Li, L., Lough, C., Replogle, A., Bristow, D., Landers, R., & Kinzel, E. (2017), Thermal Modeling of 304L Stainless Steel Selective Laser Melting. *Solid Freeform Fabrication*, Vol. 6061, pp. 1068-1081.
- [11] Enrico Salvati (2017), Residual Stress Evaluation and Modelling at the Micron Scale (Doctoral dissertation), Trinity College.